DINAME 2019 - Proceedings of the XV International Symposium on Dynamic Problems of Mechanics,
M.A. Savi, T.G. Ritto and W.M. Bessa (Editors), ABCM, Buzios, RJ, Brazil, March 10th to 15th, 2019

Electrical Fault Detection in a Rotor Supported by Active Magnetic Bearing

Gilberto Machado da Silva [1], Robson Pederiva [2]

[1] Herminio Ometto University Center and Technology College - Arthur Azevedo - Rua Ariovaldo Silveira Franco, 567 - Jd. 31 de Março - Mogi Mirim-SP – Brasil – Zip Code: 13801005 – gilberto.silva@fatecmm.edu.br

[2] University of Campinas Faculty of Mechanical Engineering - PO box 6122, Campinas – SP – Brasil, Zip Code: 13083970 - robson@fem.unicamp.br

Abstract: The problem of failure detection applied to rotational systems with active magnetic bearing (AMB) has a special difficulty because the mechanical system equations are associated to the system control structure. The measurement of all state variables normally is not possible in real systems and the knowledge of stiffness and damping values are also difficult to be identified. In order to avoid this practical characteristic, we propose a methodology that works with the structure of the model and generates compatibility equations involving correlations between a reduced numbers of state variables. These relations are obtained by the matrix equation of Ljapunov. The faults in the system are detected by monitoring the change in the physical parameters and comparing the theoretical and estimated correlation functions. Artificial neural networks are used to map the correlations involving states that are not measured. The proposed method is applied numerically to detect and locate sensor and actuator faults.

Keywords: Fault Diagnosis, Magnetic Bearings, Rotor Dynamics, Neural Networks

INTRODUCTION

Active magnetic bearings are used in equipment in which the elimination of contact surfaces enables a very low mechanical wear, a decrease in motor consumption and the disposal of lubricants. They are suitable for the construction of sealed machines, which need to operate in a vacuum or in atmospheres subject to contamination. However, in critical conditions of operation a possible fault can lead to catastrophic consequences, leading to considerable economic losses; therefore, it is of extreme importance the use of a security system to increase its reliability of use. The faults of sensors and actuators can be prevented by the redundancy of components, doubling the sensors in operation or through touchdown bearings, which hold the rotor down, Peichao, Sahinkaya and Keogh (2012). Modern turbomachinery requires the use of simple bearings, sensors and controllers. However, in order to maintain the reliability of the equipment, it becomes necessary to use a fault detection system associated with prognosis and correction systems, called smart machines, Shweitzer, (2005).

Despite the viability of turbomachinery with magnetic bearings, few studies have addressed the use of methods of fault diagnosis in this type of system. Tiwari and Chougale (2014) have applied an algorithm for estimation the dynamic parameters and residual unbalances in a flexible rotor with magnetic bearings, the algorithm is based both on the measured AMB controlling currents and rotor unbalance responses. Aenis, Knopf and Nordmann (2002) applied a fault detection algorithm in a centrifugal pump with magnetic bearings based on transfer functions and in the measurement of magnetic forces. Zhang et. al (2013) use state observers and H∞ control for compensating the delay of the response due to faults in sensors and actuators. Losh (2002), used redundant sensors to diagnose faults, using an algorithm based on the residue of measurements of the sensors with and without faults, and for faults of actuators, the coil current of the magnetic bearing is compared with a sample of currents in which the bearing can operate without destabilizing. Tsai and Lee, (2009) apply two methods for detecting faults in sensors and actuators in a system of rotor and magnetic bearing using state and parameters estimators, however, needs to combine simulation data and parameter identification to be able to identify the type of fault.

Eduardo and Pederiva (2002) developed a set of correlation equations related to the physical parameters of the system together with artificial neural networks to detect mechanical failures in a rotor with conventional bearings. Silva and Pederiva (2006) applies this formulation to a rotor supported by active magnetic bearings, with more degrees of freedom, for detecting and locating mechanical failures (loss of stiffness in the shaft) and electrical (sensor and magnetic failures) numerically. Silva and Pederiva (2007) explored mechanical faults at several rotor points using the same detection strategy. Sanches and Pederiva (2016) studies the simultaneous identification of faults by imbalance and shaft bow of the rotor, as the measured response number is lower than the total degree of freedom of the rotor, uses an auxiliary system (filter) and techniques of order reduction of the adjusted model in order to reduce the computational effort in the determination of the observability matrix, generating the additional correlations that allow the identification of the failures. Silva and Pederiva (2018), present a formulation for detection of unbalance failures in flexible rotors supported by active magnetic bearings. The model-based procedure makes use of the correlation equations, through the

matrix formulation of Ljapunov along with artificial neural networks. By the method it is possible to detect unbalance change in one or several planes simultaneously, even changing the phase angle between the disks.

In this work the same formulation is applied to identify sensor and actuator faults. The failure detection method is based on knowledge of the mathematical model structure developed for the mechanical and control system, along with the force laws of the bearings. Unbalance and white noise forces excite the system. By the analysis of the matrix equation of Ljapunov it was chosen a set of equations that describe the behavior of the system involving the physical parameters, along with the equations of correlation between the measured states. The terms of the correlation equations related to states that cannot be measured are mapped through Artificial Neural Networks, ANN. A neural network was generated for each equation of interest. At the end, the difference between the measured correlations (with failure) and the expected correlations (without failure) is calculated. Observing these differences and the equation where they are manifested, we arrive at the conclusion of the fault and the location in the system.

MATHEMATICAL MODEL AND CORRELATION FUNCTIONS

Model of Magnetic Bearing and Controller

The configuration of magnetic bearing is shown in Fig. 1. The electromagnetic force is inversely proportional to the distance, and when applying an electromagnetic force to the rotor the tendency is to be attracted to the minimum possible distance between its surface and the electromagnet.

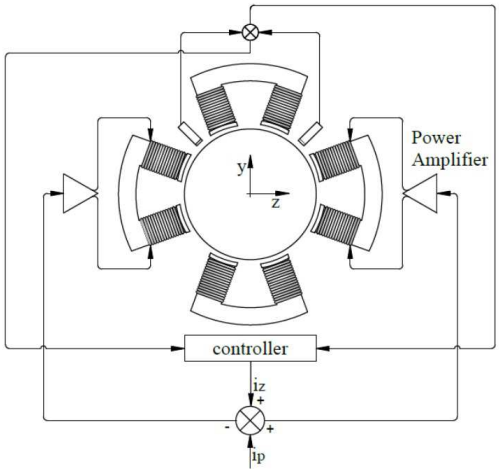

Figure 1 - Radial AMB

The force applied to the rotor in a pair of coils can be expressed by the following expression for the two half-axes:

$$\mathbf{f_m}(i,z) - \mathbf{km}\left(\frac{\mathbf{i_b}}{2}\right)^2 \tag{1}$$

In Eq. (1): z is the distance between the rotor and the stator of the bearing, ib is the bias current and km is the bearing constant depending on the air permeability, number of coils and the cross sectional area in the gap, Mendes, Cavalca and Ferreira (2012).

The law of force linearalized for small displacements around the operating point (z0, i0) and making $\mathbf{i_0 = i_p}$, for the positive semi-axis is given by:

$$\mathbf{fz} = \mathbf{4.km_z.z}(t) - \mathbf{4km_i.i_c}(t) \tag{2}$$

$$\mathbf{km_z} = \frac{\mathbf{4.km.i_b^2}}{\mathbf{g^3}} \text{ and } \mathbf{km_i} = \frac{\mathbf{4.Km.i_b}}{\mathbf{g^2}} \tag{3}$$

In Eq. (3): kmz is the constant of proportionality of force to displacement (negative spring), which is added to the mechanical stiffness matrix in the actuation planes of the magnetic bearing, and kmi the constant of proportionality of force to the current (bearing gain).

The controller is a sixth-order SISO (single in – single out), the dynamic of the control modelled in the state space is given by:

$$\dot{\mathbf{x}}(t) = \mathbf{A_c}\,\mathbf{x_c}(t) + \mathbf{B}\,\mathbf{y_c}(t) \text{ and } \mathbf{f_m} = \mathbf{A_c}\,\mathbf{x_c}(t) + \mathbf{B}\,\mathbf{y_c}(t) \tag{4}$$

In Eq. (4): Ac is the dynamic matrix of the controllers, Bc is the input matrix of the controller, yc is the input vector of the mechanical system with the ks gain of the sensor, Cc is the output matrix of the control and xc is the vector of control states with the km gain of the magnetic actuator and kp power stage gain. Since the controller is of the sixth order, there are six control states for each actuation axis.

Rotor Model and the Complete State Space Equation

The mechanical model system is composed by a rotor with shaft and four discs. The magnetic bearings and two position sensors act in the external discs, and a motor and a rotational and position sensor act in the internal discs. The model uses three shaft elements and four disc elements and sixteen degrees of freedom, being two displacements (y, z) and two rotations (θ, ϕ) for each disc, Fig. (2).

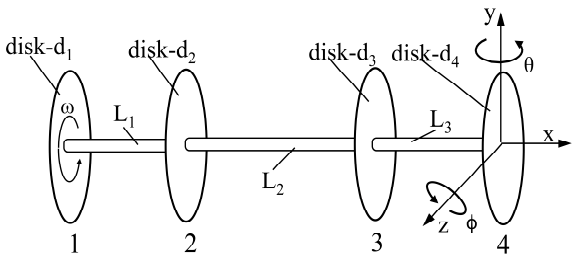

Figure 2 – Mechanical model of the system

The mechanical model can be represented by the following differential equation:

$$\mathbf{M}\ddot{\mathbf{q}}(\mathbf{t}) + \mathbf{G}\dot{\mathbf{q}}(\mathbf{t}) + \mathbf{K}\mathbf{q}(\mathbf{t}) = \mathbf{f}(\mathbf{t}) \tag{5}$$

In Eq. (5): M is the mass and inertia matrix of the discs and shaft, G is the gyroscopic effect and damping matrix, K is the stiffness matrix of the shafts and negative spring of the magnetic bearing and f(t) is the vector of external forces, which includes magnetic force, unbalanced forces and white noise. The vector q(t) represents the displacement and rotations of the system:

$$\mathbf{q}(\mathbf{t}) = [\mathbf{y}_1 \quad \mathbf{y}_2 \quad \mathbf{y}_3 \quad \mathbf{y}_4 \quad \phi_1 \quad \phi_2 \quad \phi_3 \quad \phi_4 \quad \mathbf{z}_1 \quad \mathbf{z}_2 \quad \mathbf{z}_3 \quad \mathbf{z}_4 \quad \theta_1 \quad \theta_2 \quad \theta_3 \quad \theta_4]^{\mathbf{T}} \tag{6}$$

The equation in the state space of the mechanical system is given by:

$$\dot{\mathbf{x}}_{\mathbf{m}}(\mathbf{t}) = \mathbf{A}_{\mathbf{m}}\mathbf{x}_{\mathbf{m}}(\mathbf{t}) + \mathbf{B}_{\mathbf{m}}\mathbf{fe}(\mathbf{t}) \text{ and } \mathbf{y}_{\mathbf{m}}(\mathbf{t}) = \mathbf{C}_{\mathbf{m}}\mathbf{x}_{\mathbf{m}}(\mathbf{t}) \tag{7}$$

Where:

$$\mathbf{A}_{\mathbf{m}} = \begin{bmatrix} \mathbf{Z} & \mathbf{I} \\ -\mathbf{M}^{-1}\mathbf{K} & -\mathbf{M}^{-1}\mathbf{G} \end{bmatrix} \text{ and } \mathbf{B}_{\mathbf{m}} = \begin{bmatrix} \mathbf{Z} \\ -\mathbf{M}^{-1} \end{bmatrix} \tag{8}$$

$$\mathbf{C}_{\mathbf{m}} = [\mathbf{I} \quad \mathbf{Z}] \text{ and } \mathbf{x}_{\mathbf{m}}(\mathbf{t}) = \begin{bmatrix} \mathbf{q}(\mathbf{t}) \\ \dot{\mathbf{q}}(\mathbf{t}) \end{bmatrix} \tag{9}$$

In Eq. (9): A_m is the dynamic matrix, B_m is the input matrix, C_m is the output matrix, y_m is the mechanical state vector that can be measured and $x_m(t)$ is the state vector of the mechanical system. Z is matrix of zeros, I represents the identity matrix and the points indicate the differentiation with respect to time.

From de Eqs. (4) and (7) the state space equation of the complete system is given by:

$$\dot{\mathbf{x}}_{\mathbf{f}}(\mathbf{t}) = \mathbf{A}_{\mathbf{f}}\,\mathbf{x}_{\mathbf{f}}(\mathbf{t}) + \mathbf{B}_{\mathbf{f}}\mathbf{f}(\mathbf{t}) \tag{10}$$

Where:

$$\mathbf{A}_{\mathbf{f}} = \begin{bmatrix} \mathbf{A}_{\mathbf{m}} & \mathbf{B}_{\mathbf{m}}\mathbf{C}_{\mathbf{c}} \\ \mathbf{B}_{\mathbf{c}}\mathbf{C}_{\mathbf{m}} & \mathbf{A}_{\mathbf{c}} \end{bmatrix},\ \mathbf{B}_{\mathbf{f}} = \begin{bmatrix} \mathbf{B}_{\mathbf{m}} \\ \mathbf{zeros} \end{bmatrix} \text{ and } \mathbf{x}_{\mathbf{f}} = \begin{bmatrix} \mathbf{x}_{\mathbf{m}} \\ \mathbf{x}_{\mathbf{c}} \end{bmatrix} \tag{11}$$

In Eq. (11): Af is the dynamic matrix of the complete system, Bf is the input matrix, and xf is the complete vector in the state space in closed loop, formed by the mechanical state xm and control state xc.

Correlation Functions and Artificial Neural Networks

Considering the invariant system with stationary entries. In these conditions, the correlation functions assume constant values in time and depend only on the time lag τi, given by:

$$\mathbf{R}\,\mathbf{x_f}(\tau_i) = \varepsilon\{\mathbf{x_f}(\mathbf{t})\mathbf{x_f^T}(\mathbf{t}+\tau_i)\} \tag{12}$$

Replacing the solution of Eq. (10) in Eq. (12), we have:

$$\mathbf{A_f Rx_f} + \mathbf{Rx_f A_f^T} + \mathbf{B_f Rx_n x_f} + \mathbf{Rx_f x_n B_f^T} = 0 \tag{13}$$

The Eq. (13) is called matrix equation of Ljapunov for linear stationary systems and is the basis for the development of the fault diagnosis method proposed in this work, where:

$$\mathbf{Rx_f} = \begin{bmatrix} \mathbf{Rx_m x_m} & \mathbf{Rx_m x_c} \\ \mathbf{Rx_c x_m} & \mathbf{Rx_c x_c} \end{bmatrix},\ \mathbf{Rx_n x_f} = \begin{bmatrix} \mathbf{Rx_n x_m} & \mathbf{Rx_n x_c} \end{bmatrix} \text{ and } \mathbf{Rx_f x_n} = \begin{bmatrix} \mathbf{Rx_m x_n} \\ \mathbf{Rx_c x_n} \end{bmatrix} \tag{14}$$

In Eq. (14): Rx_mx_m is the matrix of correlations between the mechanical states, Rx_mx_c is the matrix of correlations between the mechanical states and states of control , Rx_cx_m is the matrix of correlations between the states of control and mechanical states, Rx_cx_c is the matrix of autocorrelations between the states of control, Rx_nx_m is the matrix of correlations between the unbalances and mechanical states, Rx_nx_c is the matrix of correlations between the unbalances and states of control, Rx_mx_n is the matrix of correlations between the mechanical states and unbalances and Rx_cx_n is the matrix of correlations between the states of control and unbalances.

From the evolution of Eq. (13) were chosen 4 equations related to the mechanical states z1 and z4 and the control states Z1c and z4c. The terms difficult to be measured were excluded and the correlations that could be measured were placed as inputs in the neural network. The isolated terms in each neural network output corresponding to each selected compatibility equation are shown in Tab.1.

Table 1. – Mechanical and electrical parameters of the Neural Networks

State	Node	Inputs	Output	Network
z1	1	$\mathbf{R\dot{z}_1z_1}, \mathbf{R\dot{z}_1\dot{z}_1}, \mathbf{Rz_{11c}z_1}, \mathbf{Rz_{12c}z_1}, \mathbf{Rz_{13c}z_1}, \mathbf{Rz_{14c}z_1}$	$\mathbf{Rz_1z_1}$	A1
z4	4	$\mathbf{Rz_3z_4}, \mathbf{R\dot{z}_4z_4}, \mathbf{R\dot{z}_4\dot{z}_4}, \mathbf{Rz_{41c}z_4}, \mathbf{Rz_{42c}z_4}, \mathbf{Rz_{43c}z_4}, \mathbf{Rz_{44c}z_4}$	$\mathbf{Rz_4z_4}$	A4
z1c	1	$\mathbf{Rz_{11c}z_1}, \mathbf{Rz_{12c}z_1}, \mathbf{Rz_{13c}z_1}, \mathbf{Rz_{14c}z_1}, \mathbf{Rz_{15c}z_1}$	$\mathbf{Rz_1z_1}$	A1c
z4c	4	$\mathbf{Rz_{41c}z_4}, \mathbf{Rz_{42c}z_4}, \mathbf{Rz_{43c}z_4}, \mathbf{Rz_{44c}z_4}, \mathbf{Rz_{45c}z_4}$	$\mathbf{Rz_4z_4}$	A4c

The autocorrelations of output of architectures A1, A4, A1c and A4c were trained for the system without fault. The comparison between the output without and with fault is made by calculating the mean square deviation (MSD), given by:

$$\mathbf{MSD} = \left(\frac{1}{\mathbf{N}} \sum_{\mathbf{i}=1}^{\mathbf{N}} (\mathbf{Rx_f} - \overline{\mathbf{Rx_f}})^2 \right)^{\frac{1}{2}} \tag{15}$$

In Eq. (15): $\mathbf{Rx_f}$ is the autocorrelation of output of the network with fault, $\overline{\mathbf{Rx_f}}$ is the autocorrelation of output of the expected network without fault and N is the number of training data.

The neural network used has one input layer, the intermediate layer with ten neurons. We simultaneously measured all signs of the position sensors (y1, y4, z1 and z4) and the states of control in the direction Z1c (Z11c, Z12c, Z13c, Z14c and Z15c) and direction Z4c (Z41c, Z42c, Z43c, Z44c and Z45c) in the time domain, in the fixed rotation. Figure 3, shows the network model (A1) used.

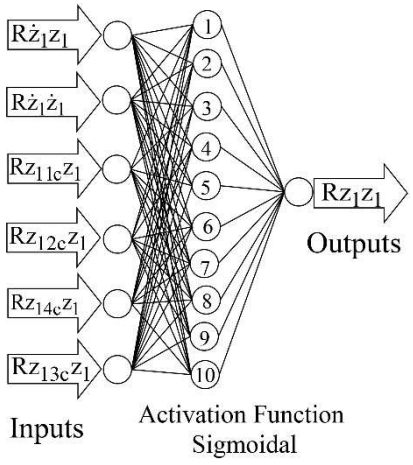

Figure 3 – Artificial Neural Network - A1

RESULTS

The time domain response of the system was obtained through MatLab - Simulink software. The Simulink model is essentially made of a block consisting of space of mechanical states equations, Eq. (7), whose output are the displacements y1, z1, y4 and z4 that pass through the gains of the sensors and feed the four blocks composed by the equations of Eq. (4); their outputs pass through the bearing gains and power stage that feedback with the magnetic force in each direction of actuation of the magnetic bearing. The system is excited by external unbalance force and white noise. The mechanical states y1, y2, y3, y4, z1 z2, z3 and z4 are obtained simultaneously and the six control states in the direction Z1c and in the direction Z4c in fixed rotation of 3000 RPM. The failure-free system parameters are listed in Tab. 2.

The system was initially considered to have a residual unbalance of 0.1 g at zero degrees in the unbalance radius of 25 mm on all disks. Correlation functions were calculated and these results were used to train the neural networks. The Levenberq Marquart algorithm was used for training the networks, adjusted for the following characteristics: sigmoidal activation function, admissible global error 10^{-6} and learning rate 10^{-4}. For the training of the networks the noise-free system was considered, the correlations were calculated by the expansion of Eq. (13) and the inputs and outputs for the neural networks shown in Tab. 1, were obtained.

Table 2. – Physical properties of the rotor and AMB's.

Disks	Parameter	Value	Unit
Mass	md	8.80 10-2	kg
Moment inertia	Id	3.10 10-5	kg.m2
Polar moment of inertia	Ip	6.02 10-5	Kg.m2
Shaft	Parameter	Value	Unit
Length	L1,L2,L3	0.150	m
Cross section	Ashaft	1.57 10-5	m2
Moment of inertia of area	Ie	5.10 10-11	m4
AMB's	Parameter	Value	Unit
Gain of the sensor	ks	1900	V/m
Gain of the power amplifier	kp	-0.25	A/V
Gain of the bearing	km	8	N/A
Negative spring	kz	-2450	N/m
Bias current	ib	0.307	A
Air gap	g	10-3	m

For the training of the networks the noise-free system was considered. Several magnitudes of white noise were added to the system in order to test the ability to map the networks in the presence of noise. The white noise magnitude was added based on the percentage of the RMS value of the unbalance force. The mean square error MSD, Eq. (15) which relates the outputs of the fault and faultless networks was used to compare the different levels of white noise, the results of which are shown in Tab. 3.

Table 3 – Mean square deviation without fault and with white noise

	MSD [%]			
White noise level	A1	A4	A1c	A4c
10%	0.222	0.002	0.690	0.759
20%	0.282	0.021	0.930	0.821
30%	0.213	0.051	0.576	0.658

It is interesting to note that with the addition of white noise at different levels, the MSD parameter did not change significantly. The simulations for the detection of electrical failures were made considering the level of 30% of white noise and rotation of 3000 RPM.

Sensor Fault

The change in the parameters of the sensor was imposed by changing the ks_{z1} sensor gain, decreasing from 19000 V/m to 16000 V/m, resulting in a loss of sensitivity of approximately 15% compared to condition without failure. The procedure was repeated making the same change in ks_{z4} sensor gain and in the sensors ks_{z1} and ks_{z4} simultaneously.

The same procedure was now performed by changing the gains of sensors from 19000V/m to 13000V /m, which represents a loss of about 30% in the sensitivity of the sensor.

For all cases was calculated the MSD, Eq. (15) for neural networks with architectures A1, A4, A1c and A4c. The results are shown in Tab.4.

Table 4 – Sensor fault– rotation 3000 RPM - with white noise

Sensor fault						
Gain	Position	A1	A4	A1c	A4c	MSD [%]
19000 V/m	ksz1	2,51	1,34	45, 9	4,06	
para	ksz4	1,29	3,10	7,08	47, 88	
16000V/m	ksz1 and ksz4	2,41	1,95	40, 53	45, 72	
19000 V/m	ksz1	2,45	0,68	62, 34	3,09	
para	ksz4	0,67	3,21	6,75	59, 13	
13000V/m	ksz1 and ksz4	3,29	2,98	60, 78	55, 92	

In the Tab. 4 the MSD error rate is higher for A1c network architecture, which is related to the state control z1c, being more predominant in the network. The same happened to the network A4c, which is related to the control state z4c. The index MSD is significant in the networks A1c and A4c, related to the states z4c and z1c respectively. In the case where fault imposed is the same, and the magnitude of the failure is greater the method is sensitive to this change.

It can be noted as well that the architecture of the networks A1 and A4, which are related to the mechanical parameters showed no significant change, indicating that the failure is of electrical type.

Bearing Fault

The bearing failures were imposed by changing the the coil current of bearings for the axes z1c and z4c. The current was varied from 0.307 A to 0.250 A, meaning a loss of approximately 20% in the current in one axis, causing a loss in gain of the bearing km_{y1} and km_{y4} by the same proportion, Eq. (3), and approximately 35% in the value of negative spring.

The same procedure was now performed by changing coil current of the bearing axis for the axes and z_{1c} and/ z_{4c} was varied from 0.307 A to 0.204 A, meaning a loss of approximately 35% in the current in one axis, causing a loss in gain of the bearing km_{y1} and km_{y4} by the same proportion, Eq. (3), and approximately 50% in the value of negative spring.

This decrease of current gain and consequently the gain of the magnetic actuator changes the parameters of stiffness, damping and actuation force of the bearing. Table (5) shown the results of applying this fault in the z direction of the bearing 1 and of the bearing 4, as of the bearing 1 and 4 together. The differences between the autocorrelations present at the outputs of the networks proposed for the failure condition and the system without failure are shown by the index MSD.

Table 5 – Bearing fault– rotation 3000 RPM - with white noise

Bearing fault						
Value	Position	A1	A4	A1c	A4c	MSD [%]
350 mA	iz_{1c}	24,98	4,25	36, 01	3,12	
Para	iz_{4c}	2,54	20,41	2,61	37, 76	
250 mA	iz_{1c} and iz4c	26, 87	18,33	35, 13	37, 76	
350 mA	iz_{1c}	31,82	3,91	45,07	5,06	
Para	iz_{4c}	3,98	28,79	4,07	48,96	
204 mA	iz_{1c} and iz4c	27,41	25,16	46,84	42,95	

In Tab. 5 the MSD error index is higher for the network architectures A1 related to the negative spring km_{z1} which is related to the mechanical state z1 together with an increase in the architecture A1c related to the control direction z1c, related to the gain the actuator magnetic km_{z1}. The same occurred for the networks A4 and A4c that are related to the direction of action z4. The MSD index is significant in the networks A1, A4, A1c and A4c related to the states z1, z4, z1c and z4c, respectively, when failure was imposed for both controls. Although the failure imposed is the same, the amount of change of current in the bearing was higher, and the method was sensitive to this change, indicating the source correct fault condition.

CONCLUSION

The fault detection method was developed based on the matrix equation of Ljapunov and artificial neural networks and applied to a flexible rotor with active magnetic bearings.

By the method used it was possible to detect sensor gain faults and faults in the coil current of the bearing, where it is not necessary to know the values of the model parameters, electrical or mechanical, but only the model structure.

Considering that many states are not possible of being measured due to the restriction imposed by the location of the drive motor or instrumentation, however the results were quite satisfactory, since they are mapped by the neural network.

Networks related to mechanical failures did not change significantly for the cases studied, indicating the correct fault diagnosis of electrical origin and the method is insensitive to the addition of white noise at the entrance, not taking this factor as possible fault

It was possible to separate the failure related to the change in the sensor gain from the coil current failure, because the error index appears in a different way related to the neural networks.

Experimental studies are being provided to exploiting this failures in the real case.

ACKNOWLEDGMENTS

The authors would like to thank CAPES, CNPq and grant # 2015/20363-6 from the São Paulo Research Foundation (FAPESP) for the financial support to this research**.**

REFERENCES

Aenis, M., Knopf, E., Nordmann, R., 2002, "Active magnetic bearing for the identification and fault diagnosis in turbomachinery", Mechatronics, vol. 12, pp.1011-1021.

Eduardo A. C.,Pederiva R., 2002, "Parameter Monitoring of a Rotor System Excited by Stochastic Forces", Proceedings of 6th International Conference on Rotor Dynamics, Sidney, Australia, pp. 310-317.

Losh F., (2002), "Detection and Correction of Actuator and Sensor Faults in Active Magnetic Bearing Systems", Proceedings of 8th International Symposium on Magnetic Bearing, Mito, Japan, pp.113-118.

Mendes, R. U., Cavalca, K.L., Ferreira, L.O.S., 2012, "Analysis of a Complete Model of Rotating Machinery Excited by Magnetic Actuator System", Proceedings of the Institution of Mechanical Engineers, Part C: Journal of Mechanical Engineering Science, Vol. 227, pp. 48-64.

Peichao, L., Sahinkaya, M. N., Keogh, P.S., 2012, "Active Magnetic and Touchdown Bearings to Encourage Re-Levitation form a Persistent Contact Condition". Proceedings of 13th International Symposium on Magnetic Bearing, Arlington, Virginia, USA, pp. 13-19.

Sanches F.D., Pederiva, R., (2016), "Theoretical and experimental identification of the simultaneous occurrence of unbalance and shaft bow in a Laval rotor", Mechanism and Machine Theory, Vol. 101, pp. 209–221.

Silva, G.M.,Pederiva, R., 2018, "Unbalance Identification in a Rotor Supported by Active Magnetic Bearing", Proceedings of 10th International Conference on Rotor Dynamics , Rio de Janeiro, Brazil, Vol. 01, pp. 82-96.

Silva. G. M.,Pederiva, R., 2007, "Mechanical Fault Diagnosis in a Flexible Rotor through Correlations Functions and Artificial Neural Network", Proceedings of 12th International Symposium on Dynamic Problems of Mechanics, Ilhabela, Brazil.

Silva, G. M.,Pederiva, R., 2006, " Diagnosis in a Rotor Supported by Active Magnetic Bearings", Proceedings of 7th International Conference on Rotor Dynamics, Vienna, Austria, pp. 25-28.

Schweitzer, G., 2002, "Active Magnetic Bearing - Chances and Limitations", Proceedings of Sixth International Conference on Rotor Dynamics, Sydney, Australia, pp. 1-14.

Tiwari R., Chougale, A., 2014, "Identification of bearing dynamic parameters and unbalance states in a flexible rotor system fully levitated on active magnetic bearings", Mechatronics, Vol. 24, pp. 274-286.

Tsai C., King Y. H., Lee R. M., 2009, "Fault Diagnosis for Magnetic Bearing", Mechanical Systems and Signal Processing, Vol.3, Issue 4, pp. 1339 - 1351.

Zhang Y. Y., Zhang J. L., Xiao, Y. L., Xin. P.G., 2013, "Sensor/Actuator Faults Detection for Networked Control Systems via Predictive Control". International Journal of Automation and Computing, Vol. 10, No. 3, pp.173 – 180.

RESPONSIBILITY NOTICE

The authors are the only responsible for the printed material included in this paper.